JEM Journal of Experimental Medicine

ARTICLE

Stability and heterogeneity in the antimicrobiota reactivity of human milk-derived immunoglobulin A

Chelseá B. Johnson-Hence[1,2], Kathyayini P. Gopalakrishna[1], Darren Bodkin[1], Kara E. Coffey[1,3], Ansen H.P. Burr[1,4], Syed Rahman[4,5], Ali T. Rai[1], Darryl A. Abbott[1], Yelissa A. Sosa[1], Justin T. Tometich[1], Jishnu Das[4,5], and Timothy W. Hand[1,4]

Immunoglobulin A (IgA) is secreted into breast milk and is critical for both protecting against enteric pathogens and shaping the infant intestinal microbiota. The efficacy of breast milk–derived maternal IgA (BrmIgA) is dependent upon its specificity; however, heterogeneity in BrmIgA binding ability to the infant microbiota is not known. Using a flow cytometric array, we analyzed the reactivity of BrmIgA against bacteria common to the infant microbiota and discovered substantial heterogeneity between all donors, independent of preterm or term delivery. Surprisingly, we also observed intradonor variability in the BrmIgA response to closely related bacterial isolates. Conversely, longitudinal analysis showed that the antibacterial BrmIgA reactivity was relatively stable through time, even between sequential infants, indicating that mammary gland IgA responses are durable. Together, our study demonstrates that the antibacterial BrmIgA reactivity displays interindividual heterogeneity but intraindividual stability. These findings have important implications for how breast milk shapes the development of the preterm infant microbiota and protects against necrotizing enterocolitis.

Introduction

Breast milk is acknowledged by the World Health Organization and American Academy of Pediatrics as the best source of nutrition for infants (Sobti et al., 2002). Breast milk contains multiple bioactive components, including antibodies, that both prevent infection and aid in the proper installation of the infant microbiota (Gopalakrishna and Hand, 2020; Le Doare et al., 2018; Walker and Iyengar, 2015). IgA, IgG, and IgM antibodies are all found in breast milk, but IgA is dominant, making up over 90% of the antibody secreted in the mammary gland. One reason for this is that during pregnancy, IgA-producing B cells travel from the intestine to the mammary gland, indicating that IgA secreted into milk is an effort to transfer maternal mucosal immunity to the infant (Lindner et al., 2015; Wilson and Butcher, 2004). During B cell production, IgA is often dimerized by the J-chain, which promotes binding and transcytosis of IgA by the polymeric glycoprotein Ig receptor that upon secretion remains bound to IgA as "secretory factor" (SF; Hand and Reboldi, 2021). SF-bound secretory IgA (SIgA) is protected against proteolytic cleavage in the intestine, substantially increasing the half-life and functionality of IgA at mucosal surfaces (Johansen and Kaetzel, 2011). The majority of IgA secreted into breast milk is SIgA (Rogier et al., 2014).

In addition to protecting against infection (Gopalakrishna and Hand, 2020), SIgA is important in shaping the development of the infant microbiota (Planer et al., 2016; Rogier et al., 2014). In breast-fed infants, milk is the predominant source of IgA in the first month of life, and in mice, lack of maternal IgA affects the development of the microbiota (Gopalakrishna et al., 2019; Mirpuri et al., 2014; Rognum et al., 1992). Infant formula, which lacks all immunoglobulins, is also associated with alterations in the infant microbiota and increased rates of short and long-term diseases (Dixon, 2015; Oddy, 2017). Preterm infants are particularly susceptible to diseases related to improper regulation of colonization by microbiota, like necrotizing enterocolitis (NEC; Bode, 2018; Cortez et al., 2018; Neu and Walker, 2011; Niño et al., 2016; Warner and Tarr, 2016). The incidence of NEC is significantly increased in formula-fed preterm infants, and the promotion of milk feeding in these children has reduced the incidence of this disease (Neu and Walker, 2011; Niño et al., 2016). In a cohort of milk-fed preterm infants, we have demonstrated that in the days directly preceding the development of

[1]Pediatrics Department, Infectious Disease Section, R.K. Mellon Institute for Pediatric Research, UPMC Children's Hospital of Pittsburgh, School of Medicine, University of Pittsburgh, Pittsburgh, PA, USA; [2]Department of Pediatrics, Division of Neonatal-Perinatal Medicine, University of Texas Southwestern Medical Center, Dallas, TX, USA; [3]Department of Pediatrics, Division of Allergy and Immunology, School of Medicine, University of Pittsburgh, Pittsburgh, PA, USA; [4]Department of Immunology, School of Medicine, University of Pittsburgh, Pittsburgh, PA, USA; [5]Center for Systems Immunology, School of Medicine, University of Pittsburgh, Pittsburgh, PA, USA.

Correspondence to Timothy W. Hand: timothy.hand@chp.edu.

NEC, there is a substantial reduction in the fraction of intestinal bacteria bound by breast milk–derived IgA, which is not observed in infants who do not develop the disease (Gopalakrishna et al., 2019). The majority of IgA "unbound" bacteria in preterm NEC infants come from one family: *Enterobacteriaceae*, which has previously been associated with the disease (Gopalakrishna et al., 2019; Pammi et al., 2017). Changes to IgA binding of the infant microbiota could either be caused by a shift in the composition of the microbiota or the antibacterial IgA reactivity of the breast milk. The level of heterogeneity in milk-derived IgA between individuals and over time within one mother is not well understood, but due to their intestinal origin (Lindner et al., 2015), the antibacterial reactivity of human mammary gland-resident IgA-producing B cells is likely to be highly individualized.

To measure the milk-derived antibacterial IgA response, we have developed a flow cytometric array that allows us to define the ability of antibodies to bind the surface of different bacterial isolates. Using this array, we have identified significant heterogeneity between different donors in the binding of bacterial isolates by milk-derived IgA. We also observed isolate-level variation in IgA binding within donor samples to closely related taxa of *Escherichia coli* and other species. In contrast to the interindividual heterogeneity, hierarchical clustering and principal component analysis (PCA) of longitudinally collected samples showed consistent clustering within donors, indicating that the antibacterial IgA reactivity of an individual is stable over the course of one infant. Analysis of milk samples collected over sequential siblings also revealed stability in antibacterial IgA reactivity, indicating that the B cells that secrete IgA into breast milk may be maintained long-term. Finally, we demonstrate that Holder pasteurization, which is commonly used to sterilize human donor milk, globally reduces bacterial binding by IgA. Together our data indicate that the antibacterial reactivity of milk-derived IgA is heterogeneous between individuals but also surprisingly stable, even over years of time. The temporal stability of breast milk–derived IgA reveals a potential weakness of vertical antibody transmission, where maternal antibody responses are uncoupled from infant intestinal bacterial colonization, potentially limiting BrmIgA's protective effects against infection and NEC (Gopalakrishna et al., 2019).

Results

Determining the antibacterial IgA reactivity of breast milk using a flow cytometric array

Antibacterial IgA is predominantly specific to surface antigens, and bacterial staining techniques that analyze bacterial lysates are complicated by irrelevant antibody crossreactivity against cytoplasmic proteins and nucleic acids (Slack et al., 2009). Therefore, we modified an approach described by Slack and colleagues to measure the antibacterial IgA specificity of breast milk antibodies by flow cytometry (Moor et al., 2016; Slack et al., 2009). To negate non-specific signals associated with the non-IgA components of breast milk, we isolated SIgA via passage over a streptococcal Peptide M column. Lithium dodecyl sulfate–polyacrylamide gel electrophoresis (LDS-PAGE) under reducing conditions of the Peptide M bound fraction revealed bands roughly corresponding in size to SF (~80 kD), IgA heavy chain (~60 kD), and light chain (~30 kD; Fig. S1 A; Sandin et al., 2002). J-chain (15 kD) is known to migrate slowly under LDS-PAGE electrophoresis and is the faint band running slightly below the light chain at ~25 kD (Fig. S1 A; Zikan et al., 1985). We confirmed by Western blot that each of the four components of SIgA was enriched in the Peptide M bound fraction (Fig. S1 B). To determine the specificity of an IgA-enriched breast milk sample for bacterial surface antigens, we incubated purified IgA samples on bacterial isolates individually arrayed on a 96-well plate (Fig. 1 A). Prior to flow cytometric analysis, purified breast milk–derived maternal IgA (BrmIgA) samples were normalized to rough protein content (280 nm absorbance), which corresponds to the concentration of IgA measured by ELISA (Fig. S1 C). After incubation with breast milk–derived IgA, bacteria are stained with a mixture of Syto BC and fluorescently labeled anti-human IgA. Syto BC is a mixture of bacterial cell wall permeable dyes that allow us to discriminate bacteria from similarly sized debris on the flow cytometer (Fig. 1 B). Syto BC$^+$ bacteria can then be assayed for binding by breast milk–derived IgA by assessing the relative fluorescence normalized to a background control of the same bacteria stained only with anti-human IgA secondary antibody (Fig. 1 C). Analysis of a dilution series of purified IgA samples revealed that the concentration of SIgA used to test bacterial binding (0.1 mg/ml) was saturating for the bacteria tested and was used as a standard concentration for all further experiments (Fig. S1 D). To control for non-specific binding of BrmIgA by bacteria, we tested a monoclonal IgA antibody specific to HIV against our array and found only very minimal binding, indicating that our array is measuring antibacterial IgA responses (Fig. 1 C; Yu et al., 2013). Further, binding of BrmIgA to the soil bacterium *Bradyrhizobium japonicum* demonstrated marginal signal, indicating that the breast milk–derived IgA response is focused on bacterial taxa that commonly colonize humans (Fig. 1 D; Haas et al., 2011).

Heterogeneity in breast milk–derived antibacterial IgA reactivity

After delivery, the infant microbiota goes through three main stages (Reyman et al., 2019). First, the infant's intestine becomes colonized by common facultative anaerobic bacteria such as *Enterobacteriaceae* and *Enterococcaceae*. Within the next 4 wk, these bacteria will be supplanted as the dominant taxa by *Bifidobacteria*, which use human milk oligosaccharides as a food source. 6 mo later, approximately coinciding with the introduction of solid food, there is another switch toward anaerobic *Firmicutes* and *Bacteroidetes* that assist with the digestion of complex carbohydrates. BrmIgA likely contributes to shaping microbiota colonization at all of these stages but is particularly important for controlling the early bacterial colonizers that comprise the first stage when infants don't make any of their own IgA (Gopalakrishna et al., 2019; Koch et al., 2016; Mirpuri et al., 2014; Rognum et al., 1992). Indeed, mouse pups fed by dams that lack IgA production or secretion are colonized for longer time periods with facultative anaerobes such as *Enterobacteriaceae* and *Pastereurellaceae* than IgA-secreting controls (Mirpuri et al., 2014; Rogier et al., 2014). Regulation of early

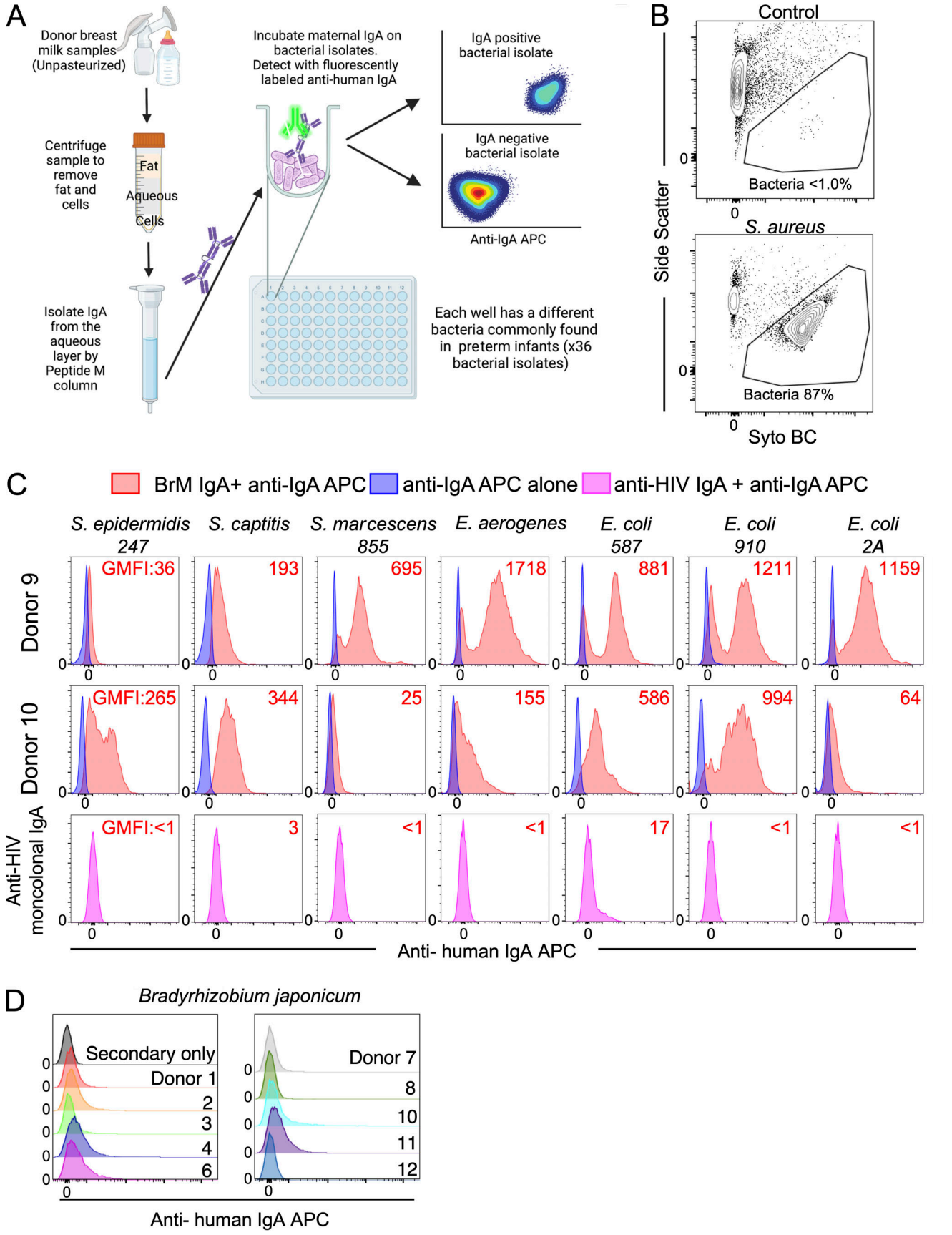

Figure 1. **A flow cytometric array for measuring the antibacterial reactivity of breast milk–derived IgA. (A)** Design of the flow cytometric array. Made with BioRender.com. **(B)** Examples of Syto BC+/SSCDim staining (2 of 3,636) used to discriminate bacteria from debris/bubbles in the flow cytometer (control

is empty well stained with Syto BC). Numbers represent the percentage of events inside the gate. **(C)** Two examples (of 101) of the magnitude of antibacterial IgA binding detected in our array comparing two donors (9 and 10) that differ in their antibacterial IgA responses. The bottom row shows the reactivity of an anti-HIV IgA antibody against the bacterial isolates (one experiment). Numbers in red represent the gMFI of that sample. **(D)** Breast milk–derived IgA reactivity, from 10 donors against the environmental bacteria *B. japonicum*. One experiment.

colonizing bacteria is especially relevant to preterm infants where increased *Enterobacteriaceae* and, in particular, IgA-free *Enterobacteriaceae* is associated with the development of NEC (Gopalakrishna et al., 2019; Pammi et al., 2017). Thus, when designing the bacterial array for analyzing the antibacterial reactivity of breast milk–derived IgA, we focused on facultative anaerobes, such as *Enterobacteriaceae*, that dominate early infant bacterial colonization. Our array contained 36 individually grown and plated bacterial isolates from 13 different genera that represent the major taxa commonly found in the intestine of preterm infants. All donor samples were normalized for the input concentration of IgA. Analysis of the antibacterial IgA responses from 33 donors revealed a substantial amount of heterogeneity, with no two donors being identical (Fig. 2 A). Thus, individualized differences in the IgA^+ B cell population of the intestine driven by distinct infection and microbiota experiences likely lead to similar heterogeneity in breast milk (Bunker et al., 2017; Hapfelmeier et al., 2010; Lindner et al., 2015; Zhang et al., 2017). Comparative analysis of the normalized magnitude of BrmIgA across all bacterial isolates revealed that rather than particular donors making universally strong or weak responses against all bacterial isolates, there was substantial heterogeneity in donor binding from bacterial isolate to isolate (Fig. 2, A and B). The magnitude of IgA binding to different bacterial isolates was also evenly distributed, where normalized IgA binding for most isolates shared a similar standard deviation, though some donors had strong binding to Gram-positive bacteria (*Staphylococcus* and *Enterococcus*), while others had very little BrmIgA reactivity to these bacteria (Fig. 2, A and B). Some bacterial isolates (*Serratia marcescens 855*, *Proteus mirabilis*, and *Lactobacillus casei*) were bound by BrmIgA from a few donors (Fig. 2 B). The heterogeneity of antibacterial IgA reactivity was also demonstrated by comparison of BrmIgA responses to related isolates of *E. coli* where the magnitude of response to each isolate of *E. coli* was highly individual to the donor and could vary more than fivefold (Fig. 2 C). Species and isolate level heterogeneity in BrmIgA reactivity was also evident in responses against *Staphylococcus*, *Serratia*, *Klebsiella*, and *Enterococcus* (Fig. 2, A and B). Despite this heterogeneity, we wanted to measure whether any of the antibacterial IgA responses were correlated, such that response to one bacterium would be predictive of another. To test this possibility, we used correlation network analyses to identify statistically significant pairwise relationships between different bacteria isolates (Ackerman et al., 2018; Suscovich et al., 2020). To illustrate global relationships in IgA binding profiles across bacterial isolates, we visualized all pairwise correlations in a heatmap (Fig. 2 D), which demonstrated two clear blocks—one composed entirely of *Enterobacteriaceae* involving highly correlated profiles and the other involving relatively uncorrelated profiles. Network analyses also revealed substantial interconnection and correlated responses specific to *Enterobacteriaceae* isolates (Fig. 2 E). Specifically, three *E. coli* isolates (587, 596, and 910) share the same O and H antigens, and they are linked in Fig. 2 E, indicating the importance of these antigens to IgA reactivity. This finding is consistent with a previous discovery of a high degree of *Enterobacteriaceae* crossreactivity in blood-derived human IgA clones due to reactivity to shared surface molecules, such as lipopolysaccharide, which contains the O antigen (Rollenske et al., 2018). There were no strong correlations discovered amongst Gram-positive bacteria, even when comparing isolates of the same bacterial genus (*Staphylococcaceae*, *Enterococcaceae*; Fig. 2, D and E). Taken together, our data indicate that even though anti-*Enterobacteriaceae* IgA responses are common and broad, the breast milk–derived antibacterial BrmIgA response is quite heterogeneous from person to person. Heterogeneity in antibacterial IgA may be important to newborns where IgA binding (or lack thereof) to infant intestinal bacteria may regulate bacterial colonization.

Heterogeneity in breast milk–derived antibacterial IgA reactivity from donors who delivered preterm infants

It is not known when during pregnancy-induced mammary gland (MG) development that B cells traffic from the intestine to the MG. In mice, it predominantly occurs late in gestation or even after delivery, whereas in pigs it occurs maximally in the second trimester (Langel et al., 2019; Roux et al., 1977). If B cell traffic to the MG during the third trimester is required for optimal breast milk IgA secretion in humans, preterm delivery, which often occurs at the transition between the second and third trimesters, may affect the level and specificity of breast milk–derived IgA. Comparison of the concentration of IgA from milk samples derived from preterm mothers (gestational age 24–35 wk) and term (>37 wk) samples revealed no significant difference (Fig. 3 A). Further, BrmIgA isolated from preterm milk samples phenocopied term milk samples with regard to the heterogeneity of antibacterial reactivity (Fig. 3, B and C). Finally, PCA could not separate term and preterm samples on the basis of the antibacterial binding reactivity, indicating that, by the metrics of IgA concentration in milk and antibacterial binding, preterm and term BrmIgA are effectively indistinguishable (Fig. 3 D).

Temporal stability of antibacterial maternal IgA reactivity within one childbirth/infant

The concentration of all proteins, including BrmIgA, is highest in colostrum and then recedes to a stable point after the transition into mature milk, but whether this shift is associated with changes in the antibacterial specificity of BrmIgA is not known. For example, whether B cells traffic in and out of the mammary gland during lactation, thus changing BrmIgA reactivity, is not well understood. We tested the stability of the antibacterial

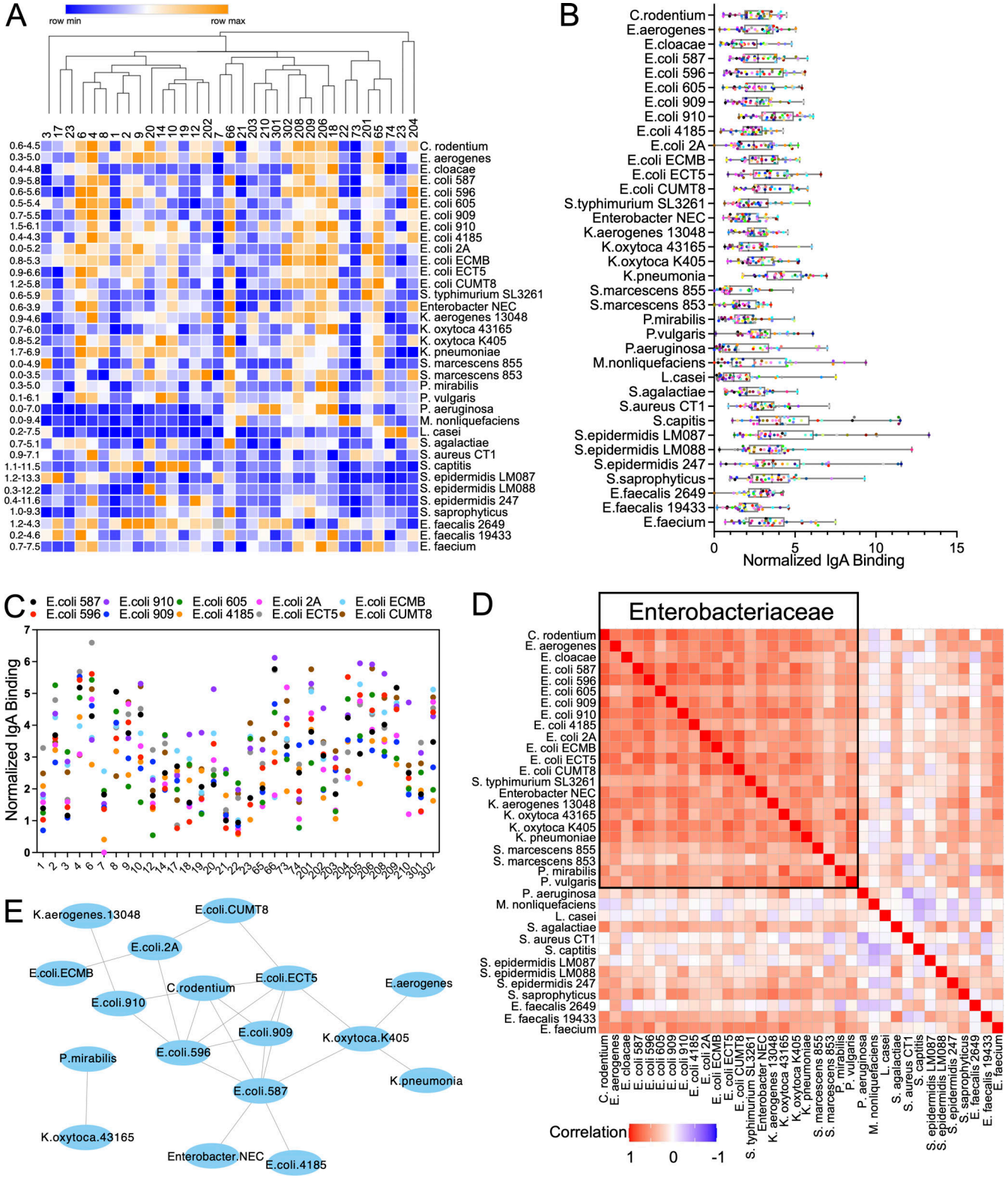

Figure 2. **Heterogeneity in the antibacterial reactivity of breast milk–derived IgA.** Donor milk samples (term infants; >37 wk gestational age) were analyzed with our flow cytometric array (Fig. 1 A). **(A)** Heat map of normalized antibacterial IgA binding affinity of different donors. Hierarchical clustering (Spearman). The range of the normalized values across each row is indicated in the left-hand column. Donor numbers indicated on top of each column. **(B)** Scatter graph showing the normalized antibacterial IgA binding values for each donor (each color represents a different donor). **(C)** Scatter graph of the normalized BrmIgA binding to different isolates of *E. coli* separated according to donors selected from the analysis in A. Donor numbers indicated on bottom of each column. **(D and E)** A correlation network analysis was performed to describe which antibacterial IgA responses were predictive. **(D)** Heat map indicating the level of correlation between different bacteria in our array. Black box drawn around *Enterobacteriaceae* family taxa. This figure is aggregate of experiments on 33 donor samples. **(E)** Network diagram indicating significantly correlated antibacterial IgA responses.

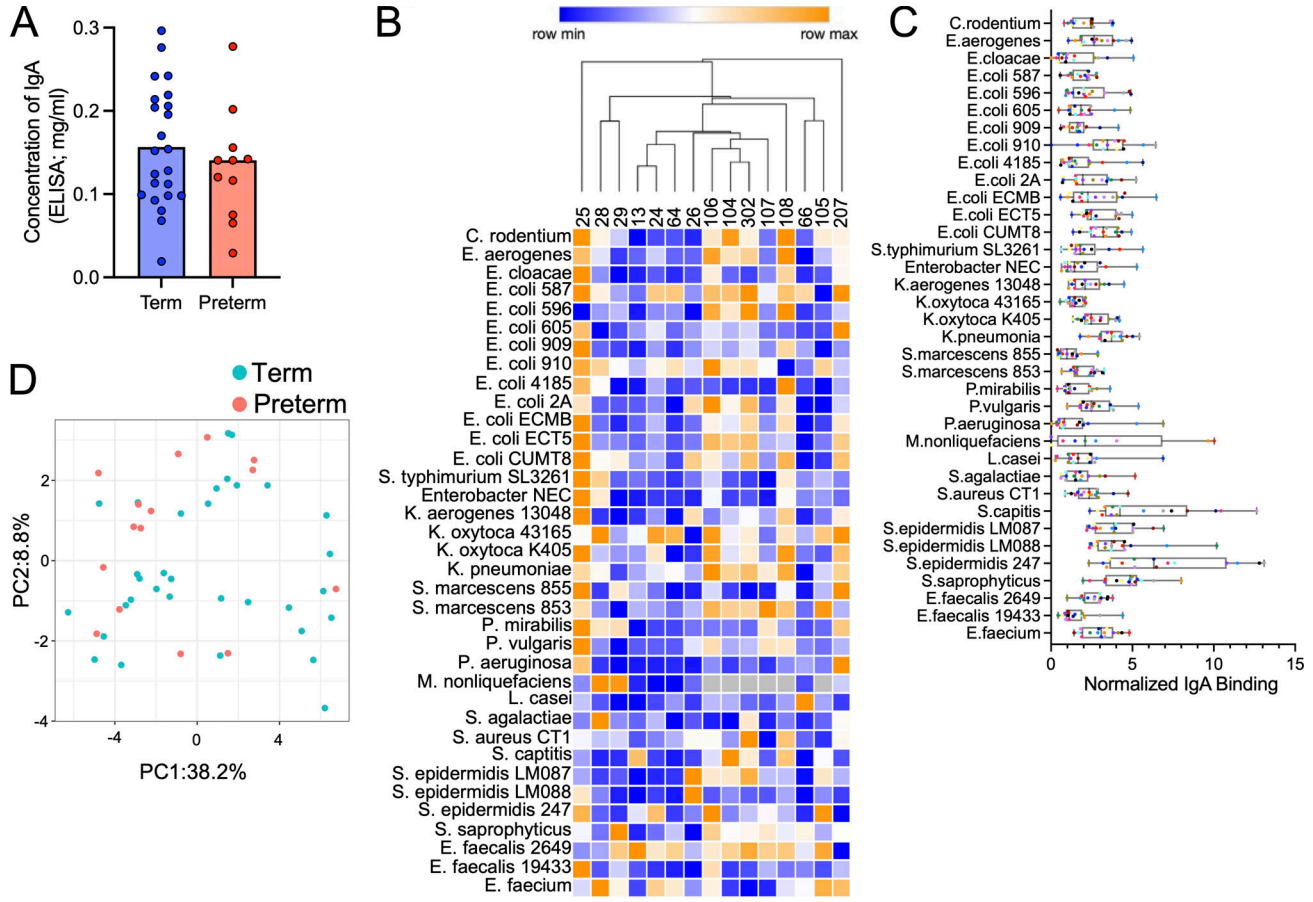

Figure 3. **Heterogeneity in breast milk–derived antibacterial IgA reactivity from donors who delivered preterm infants.** Donor milk samples (preterm infants; 24–35 wk gestational age) were analyzed with our flow cytometric array (Fig. 1 A). **(A)** Bar graph showing the concentration of IgA purified from donor milk samples from mothers of term and preterm infants (ELISA). **(B)** Heat map of normalized antibacterial binding affinity of different preterm donors (Spearman). Samples where no data were collected due to insufficient bacteria in the well are colored gray. Donor numbers indicated on top of each column. **(C)** Scatter graph showing the normalized antibacterial IgA binding values for each preterm donor (each color represents a different donor). **(D)** PCA comparing aggregate antibacterial IgA binding between preterm and term samples. This figure is an aggregate of experiments on 15 donor samples.

BrmIgA reactivity of various milk donors throughout their lactation periods, testing samples from each of the stages (colostrum, transitional, and mature). All samples were normalized for the input concentration of IgA, which is critical to account for the increased level of IgA in colostrum. Hierarchical clustering of the longitudinal samples from the seven donors revealed that in general, samples captured from the same donor over time generally clustered together, indicating that they resemble other samples from the same donor more than they resemble samples from another donor (Fig. 4 A). Longitudinal comparison of the magnitude of the IgA response against each bacterial isolate also revealed no generalizable trend toward increased or decreased antibacterial IgA binding as samples transitioned from colostrum/transitional milk to mature milk (Fig. S2). Graphical depiction of the magnitude of the response against each bacterial isolate also revealed "clustering" of samples within donor groups (Fig. 4 B; each donor is one color). Finally, PCA analysis demonstrated that the collection of samples from different donors generally formed distinct clusters (Fig. 4, C and D). Similar to data captured from individual samples of mothers of term and preterm infants (Figs. 2 and 3), longitudinal samples show significant heterogeneity between donors. Thus, while the antibacterial BrmIgA reactivity of each donor is distinct, within each mother, the antibacterial antibodies and perhaps mammary gland resident B cells are stable.

Relative stability of the breast milk antibacterial IgA through siblings

During pregnancy, B cells are induced to traffic from the small intestine and Peyer's patches to the mammary gland (Lindner et al., 2015; Ramanan et al., 2020; Wilson and Butcher, 2004). In contrast to vaccine-specific B cells, under some experimental conditions, microbiota-specific plasma B cells are replaced at a high rate in the small intestine and thus we hypothesized that the antibacterial reactivity of BrmIgA might shift substantially between sequential childbirths (Bemark et al., 2016; Hapfelmeier et al., 2010; Landsverk et al., 2017). To test this hypothesis, we acquired samples from a single donor over sequential infants and analyzed for changes in their antibacterial reactivity. Hierarchical clustering of these samples revealed that they clustered together and that samples captured after the second childbirth were most often more similar to the previous sample

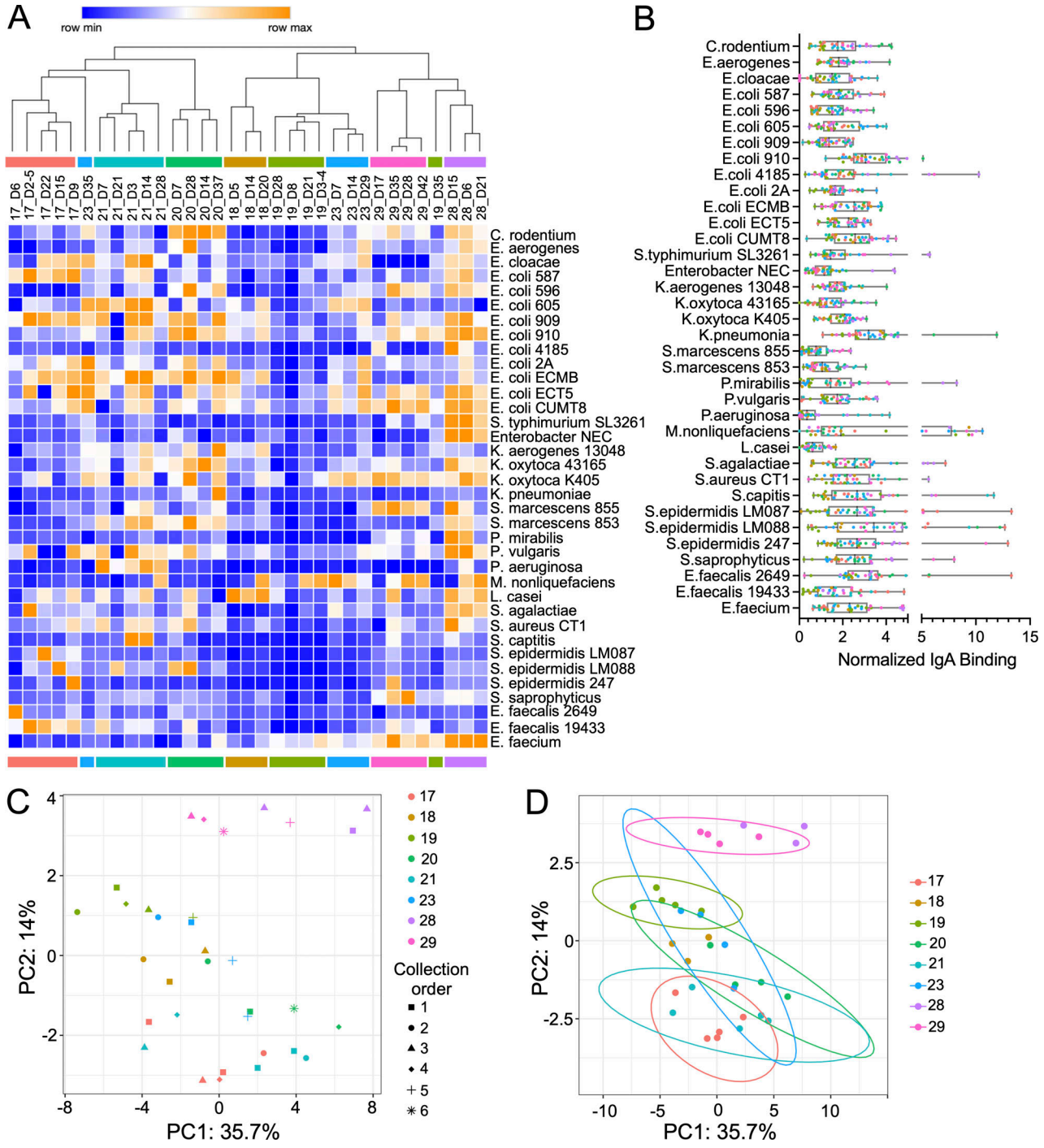

Figure 4. **Temporal stability of antibacterial maternal IgA reactivity within one childbirth/infant.** Multiple milk samples were collected from different donors over time and analyzed with our flow cytometric array (Fig. 1 A). **(A)** Heat map of normalized antibacterial binding affinity of different donors. Hierarchical clustering (Spearman) of various donors is indicated by colored bars above and below the heatmap. Date of collection indicated on heatmap: D## = number of days after delivery of sample collection. Donor numbers indicated on top of each column. **(B)** Scatter graph showing the normalized antibacterial IgA binding values for each sample from longitudinally collected donors (each color represents a different donor; from A). **(C and D)** PCA of the aggregate antibacterial IgA binding of longitudinally collected samples. Each donor colored as in A. **(C)** PCA of individual longitudinally collected samples where symbols indicate the time of collection (week after delivery). **(D)** PCA from C where ellipses indicate the maximum variance for each donor cluster along each axis. No ellipses are drawn for samples where fewer than four samples were available. This figure is an aggregate of experiments on 33 samples from eight donors.

from the same individual than any other donor (Fig. 5 A). PCA analysis confirmed the similarity of samples from sequential infants (Fig. 5 B; comparison of the location of the same-colored circles and triangles). There were individualized changes in IgA binding to different bacterial isolates between infants, but no generalizable bacterial isolate–specific trends were detected in the dataset between siblings (Fig. 5 A). However, paired analysis of each multi-infant couplet comparing the

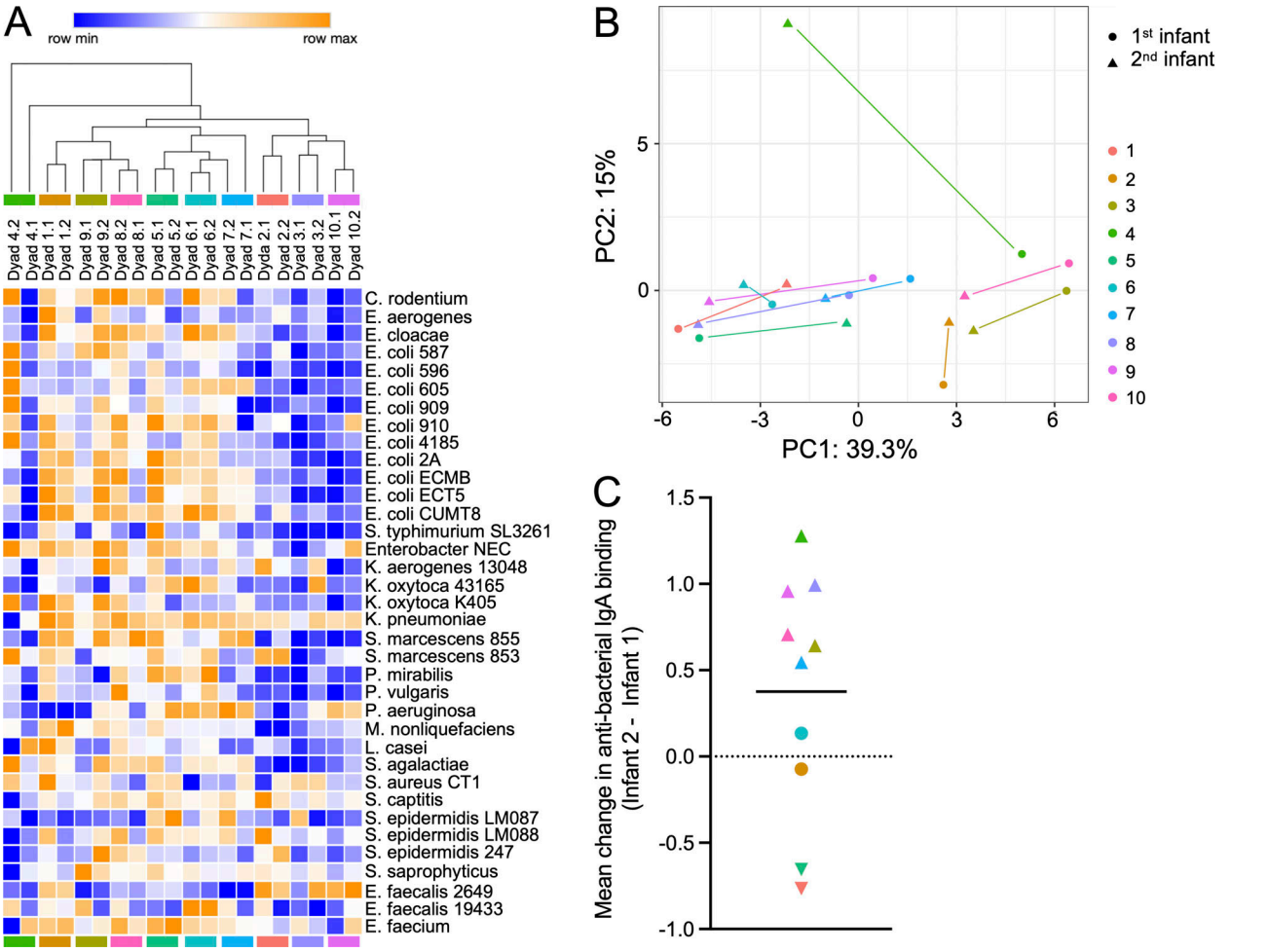

Figure 5. **Stability of breast milk–derived antibacterial IgA reactivity over the course of sibling infants.** Breast milk samples were collected from consecutive siblings and analyzed with our flow cytometric array (Fig. 1 A). **(A)** Heat map of normalized antibacterial binding affinity of different donors. Hierarchical clustering (Spearman) of various donors is indicated by colored bars above and below the heatmap that correspond to each donor. Donor numbers indicated on top of each column. **(B)** PCA of aggregate antibacterial samples where each donor is displayed in a different color (from A). The first sibling is indicated by a circle and the second sibling a triangle. Samples colored as in A. **(C)** Paired Student's *t* tests were calculated comparing the IgA binding of each donor between infant one and infant two for each bacterial taxon. The mean change ((Infant 2 – Infant 1; taxa 1) + (Infant 2 – Infant 1; taxa x))/36 (# of taxa) for each paired test was calculated and graphed. Significant increase in second infant = "up" triangle; significant decrease in second infant = "down" triangle; no statistical significance = circle. Colors are according to A. See Fig. S3 for each paired student's *t* test. This figure is an aggregate of experiments on 20 samples from 10 donors.

mean change in anti-IgA binding across all the isolates revealed that for the majority of donors antibacterial binding increased (6/10; upward pointing triangles) or stayed the same (2/10; circles) from the first childbirth to subsequent childbirths (Fig. 5 C and Fig. S3). Thus, we have observed that even between childbirths, there is stability in the antibacterial reactivity, implying either that B cells can reside in the mammary gland outside of periods of lactation or, alternatively that the same or similar B cells are trafficking from mucosal sites during each pregnancy.

Holder pasteurization reduces the bacterial binding properties of breast milk–derived IgA

Increasingly, donor milk is being used as a substitute for mother's own milk (MOM; Haiden and Ziegler, 2016). Donor milk has been shown to provide some of the benefits of MOM, including a reduction in the incidence of NEC, compared with formula-fed infants (Boyd et al., 2007; Cañizo Vazquez et al., 2019; Miller et al., 2018; Quigley et al., 2018). To prevent the transfer of potentially pathogenic bacteria, donor milk is pasteurized by the Holder method (62.5°C for 30 min). An unfortunate consequence of Holder pasteurization is the denaturation of proteins and a reduction in the function of many of the immunological components of breast milk (Adhisivam et al., 2018). Secretory IgA is particularly stable, but it has been estimated that ∼13–62% of IgA is lost by Holder pasteurization (Adhisivam et al., 2018; Lima et al., 2017; Peila et al., 2016). Here, we split four donor samples in two and compared IgA concentrations and antibacterial IgA binding between raw control and Holder pasteurized samples. ELISA for the concentration of IgA before and after pasteurization revealed a two- to three-fold drop in the concentration of IgA, consistent with published literature (Fig. 6 A).

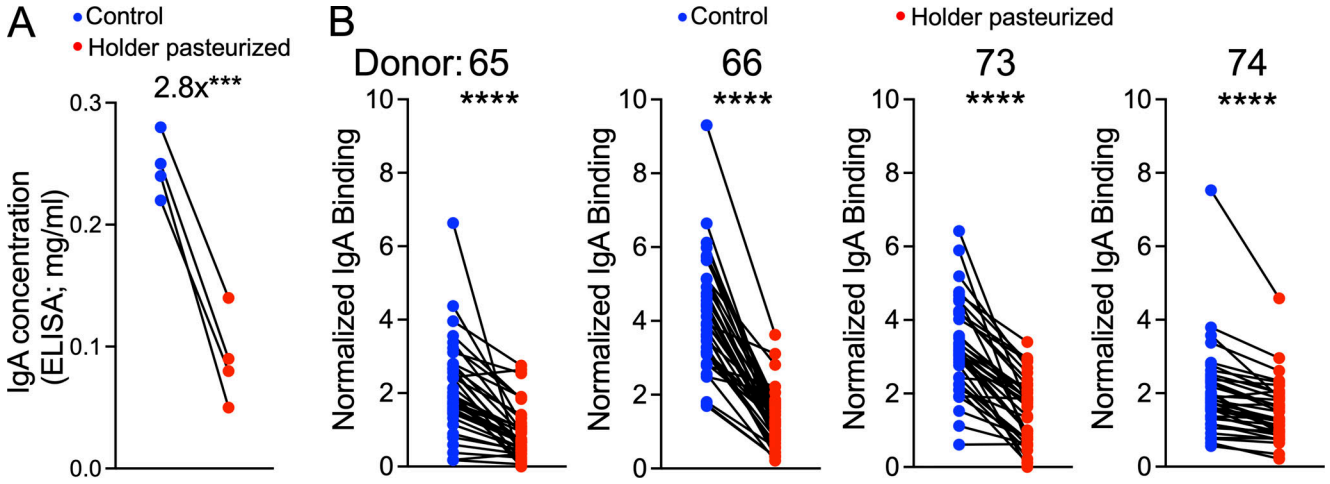

Figure 6. **Holder pasteurization reduces the bacterial binding properties of breast milk–derived IgA.** Breast milk samples from four donors were split into two where one half was pasteurized (62.5°C for 30 min) while the other was untreated as a control. IgA was then isolated from both halves and analyzed on our flow cytometric array (Fig. 1 A). **(A)** Paired Student's *t* test (***P < 0.001) of the IgA concentration (mg/ml) of control (blue) and pasteurized samples (red), as measured by ELISA. **(B)** Paired Student's *t* tests comparing control (blue) and Holder pasteurized (red) milk samples from the same donor. Each dot represents a different bacterial taxon. ****P < 0.0001. This figure is an aggregate of experiments on four donor samples.

Critically, after normalizing for protein content between paired pasteurized and control samples, we still detected an additional reduction in BrmIgA antibacterial binding responses to most isolates assayed (Fig. 6 B). LDS-PAGE and Western Blot analysis of the components of SIgA (heavy chain, light chain, J-chain, and SF), before and after pasteurization revealed no gross differences, thus the loss offunctionality of soluble SIgA after pasteurization is likely due to more subtle shifts in the tertiary structure that affect antigen binding (Fig. S4).

Discussion

Here, we demonstrate that the antibacterial reactivity of IgA in breast milk is heterogeneous between individuals but stable over time, both within one infant and over sequential childbirths. We did not find any appreciable difference in IgA content or functionality between preterm and term mothers. Additionally, we found that Holder pasteurization generally reduces the ability of breast milk–derived BrmIgA to bind bacteria, regardless of the identity of the bacteria.

A limitation of our study is the lack of obligate anaerobic bacteria within our flow cytometric array. We focused upon the facultative anaerobes that dominate the early colonization period of the infant because there is evidence that this is a critical time when BrmIgA is necessary to control microbiota colonization (Gopalakrishna et al., 2019; Mirpuri et al., 2014; Rognum et al., 1992), and that failure to control facultative anaerobes (*Enterobacteriaceae*, *Enterococcaceae*, *Streptococcaceae*, etc.) is related to the development of NEC and other infant diseases (Flannery et al., 2021; Lin et al., 2022; Olm et al., 2019; Warner and Tarr, 2016). Obligate anaerobes are also problematic substrates for our flow cytometric array, which requires multiple staining and centrifugation steps difficult to perform in an anaerobic chamber, and we are concerned that exposure to oxygen might kill or modify the bacteria leading to misleading results. A second important limitation is that while our array is built from bacterial isolates commonly found in preterm infant intestines (except *Salmonella typhimurium*), it is highly unlikely that these bacteria represent the bacterial isolates found in either the donor's or infant's intestines. Thus, we cannot determine whether differences in IgA reactivity detected in our array are reflected in the reactivity to infant intestinal bacteria. In the future, we hope to develop single-bacterial cell analysis tools to identify individual IgA-bound bacterial isolates within the infant's and mother's microbiota and correlate these with BrmIgA antibacterial reactivity.

It is not surprising that each donor in our study possessed a distinct collection of antibacterial antibodies as this is likely the result of distinct life histories with regard to gastrointestinal infection and microbiota composition. Interestingly, we observed differences in the ability of individual donors to bind different isolates from the same species of bacteria. T cell–dependent IgA-producing B cells are more likely to be targeted to bacterial surface proteins and less likely to be specific to repetitive structures on the bacteria's surface. Thus, our findings support the hypothesis, derived from experiments in mice, that the majority of MG-resident IgA-producing B cells are the product of T cell–dependent activation (Bunker et al., 2017). We hypothesize that the specificity of milk-derived IgA is skewed toward heterogeneous surface proteins that differ between isolates of the same species, contributing to isolate-level heterogeneity in IgA binding. Non-proteinaceous antigens (such as lipopolysaccharide) are also diverse in different bacterial isolates and are likely to contribute to the heterogeneity of breast milk–derived antibacterial reactivity. Conversely, using network analyses, we do see evidence of a correlation between breast milk–derived antibacterial IgA responses directed against various *Enterobacteriaceae* family bacteria. Perhaps *Enterobacteriaceae* share surface structures to a greater degree than other bacteria we tested in our array, increasing the likelihood of IgA

crossreactivity (Rollenske et al., 2018). It is possible that if we expanded the number of Gram-positive bacteria in the array, we would see more evidence of crossreactivity, but we should note that amongst five isolates of *Staphylococcaceae*, we observed no significant correlation in antibody responses.

In contrast to the heterogeneity that we observed between donors, we observed modest heterogeneity in samples captured at different stages (from the same donor). This indicates that B cells may become established in the developing mammary gland and do not turn over to a substantial degree over the course of one infant. Indeed, the same B cell clones can be identified in breast milk samples over multiple time points (Bondt et al., 2021). This is important and underscores a key limitation of vertical antibody transmission into infants, which is that the maternal IgA response is physically separate from the target of its protective effect (infant's intestine) and thus it does not respond to either bacterial or viral colonization of the infant. This is highly relevant to diseases common to preterm infants such as NEC and sepsis, where IgA present in breast milk may help prevent invasion by the nascent microbiota (Gopalakrishna et al., 2019). However, our results indicate that in some circumstances, BrmIgA might not bind all infant intestinal bacteria, and these "holes" in antibacterial reactivity would persist throughout the breast-feeding period, allowing unbound bacteria to proliferate and colonize more effectively. Previously, we observed a drop in IgA binding of *Enterobacteriaceae* that proceed the development of NEC (Gopalakrishna et al., 2019) and our new data imply that this observation is due to a shift in the microbiota to escape from maternal IgA binding and not a change in the antibacterial IgA reactivity of the milk. Thus, for particularly at-risk preterm infants, it may be helpful to supplement breast milk with IgA known to bind the bacteria best associated with diseases like NEC.

We also observed that the antibacterial reactivity of BrmIgA was stable within one donor over sequential childbirths. This is somewhat surprising because the microbiota-specific B cells that populate the mammary gland traffic from the intestine and IgA-producing B cells in the intestine are believed to turn over at a high rate (Hapfelmeier et al., 2010). Therefore, each pregnancy should lead to the deposition of new B cells and shifts in the antimicrobiota reactivity of BrmIgA. Our results demonstrated that BrmIgA reactivity from samples collected from one donor over several years and different infants looked more similar to each other than to any other donor, implying that the same IgA-producing B cells may traffic to the mammary gland during each pregnancy or that once established in the breast tissue, B cells can remain, even after lactation has been completed. In support of this idea, the majority of donors saw their responses either stay the same or improve in subsequent pregnancies. Whether B cells reside in mammary glands outside of the period of lactation or traffic back and forth between the intestine and mammary gland is testable in rodent models.

Feeding preterm infants human milk is well described to reduce the incidence of NEC compared with infant formula. Often for preterm infants, the mother's milk production is insufficient, and thus it is becoming common to supplement the infant diet with pasteurized donor milk. Whether donor milk is as effective as MOM in protecting against NEC has not been conclusively determined (Quigley et al., 2018). Here, we demonstrate that pasteurization reduces both the amount of IgA in breast milk and the ability of BrmIgA to bind bacteria. Thus, if IgA is important for the effectiveness of donor milk in reducing NEC, one might suspect that donor milk would be less effective. Holder pasteurization also negatively affects other antibacterial proteins such as lactoferrin, which could also reduce donor milk's effectiveness (He et al., 2018; Pammi and Suresh, 2017). However, there are mitigating factors that might lessen the effects of pasteurization. First, donor milk provided to neonatal intensive care units is often a mixture of multiple donors, which almost certainly broadens the antibacterial reactivity, which could be beneficial. Second, we don't know the minimum functional amount of IgA binding to bacteria that is required to modulate intestinal colonization, partially because we do not fully understand the mechanism by which BrmIgA functions (Hand and Reboldi, 2021; Pabst and Slack, 2020; Yang and Palm, 2020). Finally, human milk oligosaccharides, which shift the neonatal microbiota by increasing *Bifidobacteria*, are almost completely unaffected by pasteurization and very likely contribute to both preventing NEC and promoting healthy infant microbiota (Bode, 2018).

Taken altogether, we have demonstrated that there is substantial heterogeneity in the antibacterial reactivity of breast milk–derived IgA. We contend that this knowledge will serve as an important starting point for future studies on how binding by BrmIgA (or lack thereof) of newly colonizing bacteria shapes their ability to invade the infant's intestine.

Materials and methods

Study design

Research objectives

Our objective was to identify the heterogeneity (or lack thereof) of breast milk–derived IgA in response to common bacteria that colonize infants early after birth (in particular preterm infants).

Research subjects

De-identified milk donors from the Human Milk Science Institute and Biobank (Pittsburgh, PA) and or Mommy's Milk Human Milk Research Biorepository (San Diego, CA).

Experimental design

We analyzed antibacterial IgA reactivity with a custom bacterial flow cytometric array, which we designed in our laboratory specifically for this purpose and is described in detail in both Fig. 1 and below in the Materials and methods section. No randomization or blinding was used for this study.

Sample size

Since this was a discovery project and we really did not know the level of heterogeneity present within the breast milk–derived antibacterial IgA reactivity, we did not perform a power analysis.

Data inclusion and exclusion

All samples that we acquired were analyzed, except samples where the IgA concentration was too low. In some cases, specific

Table 1. **Donor metadata**

Cohort	Term (PA)	Preterm (PA)	Longitudinal (PA)	Two infants (CA)	Pasteurization (PA)
Donor age (years)	32.5 ± 4.2 (29–40) (unknown for 11 donors)	32.5 ± 4.5 (19–38)	33.7 ± 4.3 (29–40) (unknown for one donor)	31.7 ± 3.9 (22–39) (includes age of first and second infant)	30.5 ± 8.3 (19–39)
Estimated gestation age of infant at delivery (weeks)	39.6 ± 1.1 (37–41)	30.7 ± 3.1 (25–35)	37.9 ± 3.4 (32–41)	38.2 ± 3.4 (25–42) (includes both infants)	36.5 ± 4.4 (30–39)
Time after delivery of sample collection (days)	74.9 ± 79.6 (14–276)	55.6 ± 100.3 (4–330)	18 ± 11.2 (3–42)	258.3 ± 157.6 (44–688) (includes both infants)	7.5 ± 1 (7–9)
Race of donor	100% Caucasian	93% Caucasian, 7% Black	100% Caucasian	20% Caucasian, 40% Black, 40% Asian	100% Caucasian
Ethnicity of donor	Unknown	Unknown	Unknown	40% Hispanic	Unknown

Errors (±) represent SD. Number in brackets indicate range. Metadata was not collected from all donors, as indicated. (PA = samples from Pittsburgh, PA; CA = samples from San Diego, CA.)

wells were omitted from our analysis if the number of bacteria in the well was insufficient for analysis (mostly *Moraxella nonliquefaciens*). No outliers were excluded. All acquired data is included in our analyses.

Replicates

Samples were processed and analyzed over many weeks, and consistent flow cytometric measurements (though heterogeneous between samples) were an important internal control that was continuously assessed. During the development of our methodology, we repeated IgA/bacterial binding assays on consecutive days with the same milk-derived IgA samples and bacterial isolates to confirm that the staining was repeatable.

Samples and protocols

Human donor milk samples

The human study protocol was deemed "Not Human Research" by the Institutional Review Board (PRO19110221; Protocol number) of the University of Pittsburgh. The majority of the deidentified donor maternal milk was acquired from the Human Milk Science Institute and Biobank of Pittsburgh, Pennsylvania. We acquired deidentified maternal milk collected over sequential childbirths (dyads) from Mommy's Milk Human Milk Research Biorepository of San Diego, CA. All donor milk samples were stored at −80°C.

Donor metadata

Donor metadata are listed in Table 1.

Immunoglobulin A extraction

To extract the IgA from milk, the donor milk was thawed at 4°C and 2 ml of the maternal milk was placed in a 2-ml Eppendorf tube. To separate the whey protein from the fat, the maternal milk was centrifuged at 16,000 *g* for 5 min at 4°C. The fat formed a layer at the top of the tube and the cells at the bottom of the tube. The whey protein was separated from the fat by carefully pipetting and filtering through a 0.22-µm syringe filter, followed by washing the 0.22 µm syringe filter with 500 µl of wash buffer (PBS). The filtered sample was then passed through a gravity flow column containing Peptide M agarose after equilibrating the column with PBS. The sample was allowed to completely enter the matrix. The columns were washed with 10 ml of 1X PBS. The column was then eluted with 10 ml elution buffer (0.1 M glycine, pH 2–3). 10 ml of 1 M Tris with a pH of 7.5 was used to neutralize the solution. The 20 ml sample was concentrated using a protein concentrator by centrifugation of the column at 3,000 RPM for 20 min at 4°C. The concentrated sample was collected in 1.5-ml Eppendorf tubes and stored at −80°C.

Immunoglobulin A quantification

Prior to running IgA samples on our array, protein content was estimated via measurement on a Nanodrop UV Spectrophotometer. The concentration of IgA in each sample was measured by ELISA (Abcam) according to the manufacturer's directions.

Protein detection

Various fractions of either protein (pre– and post–Peptide M column) were loaded onto a gradient acrylamide gel (4–15%) and separated by LDS-PAGE electrophoresis prior to staining with Coomassie Blue stain. Alternatively, proteins separated by weight were transferred onto nitrocellulose membranes and identified by Western Blotting. Membrane blocking and primary antibody staining were performed in TBS-Tween (0.05%) with the addition of powdered milk (anti-IgA heavy chain 1:10,000; Abcam; anti-light chain [kappa] 1:1,000; Abcam; anti-J-chain 1:500; Thermo Fisher Scientific; anti-SF 1:400; Abcam).

Bacterial cultures and flow cytometric array development

We identified 13 genera commonly found within preterm infants and identified strains within the University of Pittsburgh community and ATCC collection that would be representative of the preterm infant microbiota. Bacteria were grown according to guidelines provided by ATCC or the providing investigator (see chart below) ∼18–96 h (as described below in the table). The bacteria were diluted twofold (1:2) to measure OD. 1 ml of bacterial stock was then added to a 1.5-ml Eppendorf tube. The Eppendorf tube was centrifuged at 8,000 *g* for 5 min and washed

Table 2. **Bacterial cultures**

Bacterial isolate	Source	Growth media	Time of growth	O and H antigens
Citrobacter rodentium 51459	American type Culture collection (ATCC)	Luria Bertani (LB) broth	18 h	
Enterobacter aerogenes K457	R. Kowalski (University of Pittsburgh [PITT])	LB	42 h	
Enterobacter cloacae K1535	R. Kowalski, PITT	LB	18 h	
E. coli 587	L. Harrison/J. March, PITT	LB	18 h	O25:H4
E. coli 596	L. Harrison/J. March, PITT	LB	18 h	O25:H4
E. coli 605	L. Harrison/J. March, PITT	LB	18 h	O1:H6
E. coli 909 (K746)	R. Shanks, PITT	LB	18 h	O46:H31
E. coli 910 (K1671)	R. Shanks, PITT	LB	18 h	O25:H4
E.coli 4185 (EC100D)	R. Shanks, PITT	LB	18 h	O16:H48
E. coli 2A	R. Longman, Weill Cornell	LB	18 h	H45
E. coli ECMB	Y. Belkaid, NIH; Hand, PITT	LB	18 h	O7:H7
E. coli ECT5	Y. Belkaid, NIH; Hand, PITT	LB	18 h	O22:H8
E. coli CUMT8	K. Simpson, Cornell University	LB	18 h	O46:H21
S. typhimurium (SL3261)	Y. Belkaid, NIH; Hand, PITT	LB	18 h	
Enterobacter spp. (NEC)	M. Good, University of North Carolina School of Medicine	LB	18 h	
Klebsiella aerogenes 13048	ATCC	LB	18 h	
Klebsiella oxytoca 43165	ATCC	LB	18 h	
K. oxytoca K405	R. Kowalski, PITT	LB	18 h	
Klebsiella pneumoniae	Y. Belkaid, NIH; Hand, PITT	Tryptic soy broth	18 h	
S. marcescens 855	R. Shanks, PITT	LB	18 h	
S. marcescens 853	R. Shanks, PITT	LB	18 h	
P. mirabilis	R. Kowalski, PITT	LB	18 h	
Proteus vulgaris	R. Kowalski, PITT	LB	18 h	
Pseudomonas aeruginosa 01	Y. Belkaid, NIH; Hand, PITT	LB	18 h	
Moraxella nonliquefaciens E542	R. Kowalski, PITT	LB	42 h	
L. casei 39539	ATCC	Lactobacilli MRS broth	18 h	
Streptococcus agalactiae BAA-2675	ATCC	Brain heart infusion broth	18 h	
Staphylococcus aureus CT1	Y. Belkaid, NIH; Hand, PITT	Tryptic soy broth	18 h	
Staphylococcus capitis 1931 (B1379)	R. Shanks, PITT	LB	18 h	
Staphylococcus epidermidis NIHLM087	Y. Belkaid NIH	Todd Hewitt Broth	18 h	
S. epidermidis NIHLM088	Y. Belkaid, NIH	Todd Hewitt Broth	18 h	
S. epidermidis 247 (NARSA101)	R. Shanks, PITT	LB	18 h	
Staphylococcus saprophyticus 481 (E751)	R. Shanks, PITT	LB	18 h	
Enterococcus faecalis 2649 (E286)	R. Shanks, PITT	LB	18 h	
E. faecalis 19433	ATCC	Brain heart infusion broth	18 h	
E. faecium BAA-2946	ATCC	Lactobacilli MRS broth	42 h	
B. japonicum 10324	ATCC	Yeast mannitol broth	96 h	

with 1 ml sterile 1X PBS twice. The supernatant was removed and resuspended with 1 ml of sterile 1X PBS. The bacteria were then diluted to make the final concentration of ~8 × 10^7/ml CFU. To preserve the integrity of the bacteria during the freezing process, 100 µl of glycerol was added to the dilution (1:10). 27 µl of the bacteria and glycerol mixture were then added to two wells each in a 96-well U-bottom plate, as experiment and control. The plates (containing 36 samples) were then stored at −80°C. O and H antigens were determined by sequencing (https://cge.food.dtu.dk/services/SerotypeFinder/; Joensen et al., 2015).

Bacterial cultures are listed in Table 2.

Bacterial flow assay

The bacterial plates, stored at −80°C, were thawed at room temperature and washed twice (Swinging bucket centrifuge: 4,000 RPM for 5 min) with 200 µl wash buffer (0.5% BSA [Sigma-Aldrich] in PBS-filtered through a 2.2-µm filter). The concentrated IgA from breast milk samples was thawed at 4°C and normalized to 0.1 mg/ml by diluting the sample with sterile PBS. 25 µl of the normalized IgA with 25 µl of sterile 1X PBS was added to all the bacteria in the experimental wells. For controls, 50 µl of sterile PBS was added. The plate was incubated for 1 h in dark on ice. After incubation, the plate was washed twice with 200 µl wash buffer (4,000 RPM for 5 min). All the wells in the 96-well plate were then stained with 50 l secondary antibody staining mixture of Syto BC (Green Fluorescent nucleicacid stain, Life Technologies [1:400]), APC Anti-Human IgA (Anti-Human IgA APC [Miltenyi Biotec clone REA1014, 1:50]), and blocking buffer of normal mouse serum (Thermo Fisher Scientific [1:5]). The stained samples were incubated in the dark for an hour on ice. Samples were then washed three times with 200 µl of wash buffer before flow cytometry analysis on the LSRFortessa-BD Biosciences.

For every donor, we ran a separate plate that was stained only with the Syto BC/APC antihuman IgA mix. These control samples were used as background fluorescence controls to establish positive-binding signals and normalize samples collected on different days.

Quantification and statistical analysis

Flow cytometry

All the data from flow cytometry was collected on a LSR Fortessa flow cytometer from BD Biosciences. The raw data were analyzed through the software FlowJo V10.4.2 (FlowJo). Samples were gated on SytoBC + SSCDim events as our experience with sorting and analyzing bacteria with flow cytometry has shown that this gating strategy (Fig. 1 B) limits contamination of our "bacteria" gate with debris and other bubbles. However, because (i) the SytoBC + SSCDim bacteria gate is not perfect, (ii) we are using polyclonal antibody preparations, and (iii) the bacteria itself is not homogenous due to phase/growth stage variation, bacterial IgA staining often demonstrated heterogeneous binding. Given that low (or the lack of) IgA binding may also be an important result, we capture the totality of the IgA binding in any bacteria by measuring the Geometric mean fluorescence intensity (gMFI) of SytoBC + SSCDim events. All samples are then normalized according to the following formula: Log_2 [(gMFI breast milk-derived IgA stained sample)/(gMFI of bacteria stained only with antihuman IgA APC antibody). Negative values (where the control has greater fluorescence than the stained) are set to zero.

PCA

PCA plots were made using available R packages (ggplot2) and display similarities in the percent binding of each donor sample to each bacterial taxon. Confidence ellipses demonstrate distinct groups based on multivariate t-distribution.

Correlation network analyses

We computed and visualized all pairwise Pearson correlations (of IgA binding profiles across bacterial isolates) in a heatmap using R. Significant correlations were defined using an effect size threshold of |r|>0.7 and a false discovery rate (P value adjusted for multiple comparisons using Benjamini-Hochberg multiple testing correction) threshold of <0.05. The significant correlations were visualized as a network using Cytoscape.

Statistical tests and analysis software

Heat maps were created using the MORPHEUS software tool (https://software.broadinstitute.org/morpheus/). Hierarchical clustering is by Spearman correlation. Samples collected over multiple infants were compared by either a standard or paired Student's *t* test (GraphPad PRISM 9).

Online supplemental material

Fig. S1 describes experiments related to the purification and quality control of IgA isolated from breast milk. Fig. S2 indicates the heterogeneity in BrmIgA antibacterial responses from longitudinally collected samples. Fig. S3 displays a paired analysis of infant dyads who share a mother where we collected milk samples used to feed both infants. Fig. S4 shows the effects of Holder pasteurization on components (heavy chain and light chain) of BrmIgA.

Data availability

All original flow cytometry files and gels/blots will be available at http://IMMport.org (accession #: SDY2286).

Acknowledgments

We would like to stress that we are only measuring the antibacterial IgA reactivity of breast milk samples and are not drawing conclusions on the best feeding option for any given infant. We would like to thank C. Verardi, D. O'Connor, K. Baumgartel, and the entire staff of the Mid Atlantic Mother's Milk Bank/Human Milk Science Institute and Biobank (Pittsburgh). We would also like to thank K. Bertrand and C. Chambers and the Mommy's Milk Human Milk Research Biorepository of San Diego, California (University of California, San Diego). We would like to thank L. Harrison, R. Kowalski, J. Marsh, M. Morowitz, and R. Shanks (University of Pittsburgh, Pittsburgh, PA), R. Longman (Weill Cornell Medical School, New York, NY), Y. Belkaid (National Institutes of Health, Bethesda,

MD), M. Good (University of North Carolina School of Medicine, Chapel Hill, NC), and K. Simpson (Cornell University, Ithaca, NY) for kindly providing bacterial strains and advice on strain selection. We would like to thank L. Cavacini and B. Muriuki (University of Massachusetts Medical Center, Worcester, MA) for the HIV-specific monoclonal IgA antibody. We would like to thank J. Michel and the Rangos Research Center Flow Cytometry core for assistance with running bacterial samples by flow cytometry.

This work was supported by the UPMC Children's Hospital of Pittsburgh/R.K. Mellon Institute for Pediatric Research, the National Institutes of Health (NIH, R01DK120697 to T.W. Hand and T32AI089443 to A.H.P. Burr), and a March of Dimes Innovative Challenge Grant (T.W Hand).

Author contributions: C.B. Johnson-Hence, K.P. Gopalakrishna, K.E. Coffey, D. Bodkin, and T.W. Hand conceptualized the project, developed the methodology, and designed the experiments. C.B. Johnson-Hence, K.P. Gopalakrishna, K.E. Coffey, Y.A. Sosa, D. Bodkin, D.A. Abbott, A.T. Rai, and J.T. Tometich performed the experiments. C.B. Johnson-Hence, D. Bodkin, A.T. Rai, A.H.P. Burr, S. Rahman, J. Das, and T.W. Hand analyzed the data. C.B. Johnson-Hence and T. W. Hand wrote the manuscript.

Disclosures: K.P. Gopalakrishna reported a patent for Methods of screening antibodies for treating and/or preventing necrotizing enterocolitis (NEC) issued. T.W. Hand reported personal fees from Keller Postman LLC outside the submitted work; in addition, T.W. Hand had a patent to USSN: 17/341,272 pending. No other disclosures were reported.

Submitted: 12 May 2022
Revised: 11 April 2023
Accepted: 15 June 2023

References

Ackerman, M.E., J. Das, S. Pittala, T. Broge, C. Linde, T.J. Suscovich, E.P. Brown, T. Bradley, H. Natarajan, S. Lin, et al. 2018. Route of immunization defines multiple mechanisms of vaccine-mediated protection against SIV. *Nat. Med.* 24:1590–1598. https://doi.org/10.1038/s41591-018-0161-0

Adhisivam, B., B. Vishnu Bhat, K. Rao, S.M. Kingsley, N. Plakkal, and C. Palanivel. 2018. Effect of holder pasteurization on macronutrients and immunoglobulin profile of pooled donor human milk. *J. Matern. Fetal Neonatal. Med.* 32:3016–3019. https://doi.org/10.1080/14767058.2018.1455089

Bemark, M., H. Hazanov, A. Strömberg, R. Komban, J. Holmqvist, S. Köster, J. Mattsson, P. Sikora, R. Mehr, and N.Y. Lycke. 2016. Limited clonal relatedness between gut IgA plasma cells and memory B cells after oral immunization. *Nat. Commun.* 7:12698. https://doi.org/10.1038/ncomms12698

Bode, L. 2018. Human milk Oligosaccharides in the prevention of necrotizing enterocolitis: A journey from in vitro and in vivo models to mother-infant cohort studies. *Front Pediatr.* 6:385. https://doi.org/10.3389/fped.2018.00385

Bondt, A., K.A. Dingess, M. Hoek, D.M.H. van Rijswijck, and A.J.R. Heck. 2021. A direct MS-based approach to profile human milk secretory immunoglobulin A (IgA1) reveals donor-specific clonal repertoires with high longitudinal stability. *Front. Immunol.* 12:789748. https://doi.org/10.3389/fimmu.2021.789748

Boyd, C.A., M.A. Quigley, and P. Brocklehurst. 2007. Donor breast milk versus infant formula for preterm infants: Systematic review and meta-analysis. *Arch. Dis. Child. Fetal Neonatal. Ed.* 92:F169–F175. https://doi.org/10.1136/adc.2005.089490

Bunker, J.J., S.A. Erickson, T.M. Flynn, C. Henry, J.C. Koval, M. Meisel, B. Jabri, D.A. Antonopoulos, P.C. Wilson, and A. Bendelac. 2017. Natural polyreactive IgA antibodies coat the intestinal microbiota. *Science.* 358:eaan6619. https://doi.org/10.1126/science.aan6619

Cañizo Vázquez, D., S. Salas García, M. Izquierdo Renau, and I. Iglesias-Platas. 2019. Availability of donor milk for very preterm infants decreased the risk of necrotizing enterocolitis without adversely impacting growth or rates of breastfeeding. *Nutrients.* 11:1895. https://doi.org/10.3390/nu11081895

Cortez, J., K. Makker, D.F. Kraemer, J. Neu, R. Sharma, and M.L. Hudak. 2018. Maternal milk feedings reduce sepsis, necrotizing enterocolitis and improve outcomes of premature infants. *J. Perinatol.* 38:71–74. https://doi.org/10.1038/jp.2017.149

Dixon, D.L. 2015. The role of human milk immunomodulators in protecting against viral bronchiolitis and development of chronic wheezing illness. *Children.* 2:289–304. https://doi.org/10.3390/children2030289

Flannery, D.D., E.M. Edwards, K.M. Puopolo, and J.D. Horbar. 2021. Early-onset sepsis among very preterm infants. *Pediatrics.* 148:e2021052456. https://doi.org/10.1542/peds.2021-052456

Gopalakrishna, K.P., and T.W. Hand. 2020. Influence of maternal milk on the neonatal intestinal microbiome. *Nutrients.* 12:823. https://doi.org/10.3390/nu12030823

Gopalakrishna, K.P., B.R. Macadangdang, M.B. Rogers, J.T. Tometich, B.A. Firek, R. Baker, J. Ji, A.H.P. Burr, C. Ma, M. Good, et al. 2019. Maternal IgA protects against the development of necrotizing enterocolitis in preterm infants. *Nat. Med.* 25:1110–1115. https://doi.org/10.1038/s41591-019-0480-9

Haas, A., K. Zimmermann, F. Graw, E. Slack, P. Rusert, B. Ledergerber, W. Bossart, R. Weber, M.C. Thurnheer, M. Battegay, et al. 2011. Systemic antibody responses to gut commensal bacteria during chronic HIV-1 infection. *Gut.* 60:1506–1519. https://doi.org/10.1136/gut.2010.224774

Haiden, N., and E.E. Ziegler. 2016. Human milk banking. *Ann. Nutr. Metab.* 69:8–15. https://doi.org/10.1159/000452821

Hand, T.W., and A. Reboldi. 2021. Production and function of immunoglobulin A. *Annu. Rev. Immunol.* 39:695–718. https://doi.org/10.1146/annurev-immunol-102119-074236

Hapfelmeier, S., M.A. Lawson, E. Slack, J.K. Kirundi, M. Stoel, M. Heikenwalder, J. Cahenzli, Y. Velykoredko, M.L. Balmer, K. Endt, et al. 2010. Reversible microbial colonization of germ-free mice reveals the dynamics of IgA immune responses. *Science.* 328:1705–1709. https://doi.org/10.1126/science.1188454

He, Y.M., X. Li, M. Perego, Y. Nefedova, A.V. Kossenkov, E.A. Jensen, V. Kagan, Y.F. Liu, S.Y. Fu, Q.J. Ye, et al. 2018. Transitory presence of myeloid-derived suppressor cells in neonates is critical for control of inflammation. *Nat. Med.* 24:224–231. https://doi.org/10.1038/nm.4467

Joensen, K.G., A.M. Tetzschner, A. Iguchi, F.M. Aarestrup, and F. Scheutz. 2015. Rapid and easy in silico serotyping of Escherichia coli isolates by use of whole-genome sequencing data. *J. Clin. Microbiol.* 53:2410–2426. https://doi.org/10.1128/JCM.00008-15

Johansen, F.E., and C.S. Kaetzel. 2011. Regulation of the polymeric immunoglobulin receptor and IgA transport: New advances in environmental factors that stimulate pIgR expression and its role in mucosal immunity. *Mucosal Immunol.* 4:598–602. https://doi.org/10.1038/mi.2011.37

Koch, M.A., G.L. Reiner, K.A. Lugo, L.S. Kreuk, A.G. Stanbery, E. Ansaldo, T.D. Seher, W.B. Ludington, and G.M. Barton. 2016. Maternal IgG and IgA antibodies dampen mucosal T helper cell responses in early life. *Cell.* 165:827–841. https://doi.org/10.1016/j.cell.2016.04.055

Landsverk, O.J., O. Snir, R.B. Casado, L. Richter, J.E. Mold, P. Réu, R. Horneland, V. Paulsen, S. Yaqub, E.M. Aandahl, et al. 2017. Antibody-secreting plasma cells persist for decades in human intestine. *J. Exp. Med.* 214:309–317. https://doi.org/10.1084/jem.20161590

Langel, S.N., F.C. Paim, M.A. Alhamo, A. Buckley, A. Van Geelen, K.M. Lager, A.N. Vlasova, and L.J. Saif. 2019. Stage of gestation at porcine epidemic diarrhea virus infection of pregnant swine impacts maternal immunity and lactogenic immune protection of neonatal suckling piglets. *Front. Immunol.* 10:727. https://doi.org/10.3389/fimmu.2019.00727

Le Doare, K., B. Holder, A. Bassett, and P.S. Pannaraj. 2018. Mother's milk: A purposeful contribution to the development of the infant microbiota and immunity. *Front. Immunol.* 9:361. https://doi.org/10.3389/fimmu.2018.00361

Lima, H.K., M. Wagner-Gillespie, M.T. Perrin, and A.D. Fogleman. 2017. Bacteria and bioactivity in holder pasteurized and shelf-stable human milk products. *Curr. Dev. Nutr.* 1:e001438. https://doi.org/10.3945/cdn.117.001438

Lin, Y.C., A. Salleb-Aouissi, and T.A. Hooven. 2022. Interpretable prediction of necrotizing enterocolitis from machine learning analysis of premature

infant stool microbiota. *BMC Bioinformatics*. 23:104. https://doi.org/10.1186/s12859-022-04618-w

Lindner, C., I. Thomsen, B. Wahl, M. Ugur, M.K. Sethi, M. Friedrichsen, A. Smoczek, S. Ott, U. Baumann, S. Suerbaum, et al. 2015. Diversification of memory B cells drives the continuous adaptation of secretory antibodies to gut microbiota. *Nat. Immunol.* 16:880–888. https://doi.org/10.1038/ni.3213

Miller, J., E. Tonkin, R.A. Damarell, A.J. McPhee, M. Suganuma, H. Suganuma, P.F. Middleton, M. Makrides, and C.T. Collins. 2018. A systematic review and meta-analysis of human milk feeding and morbidity in very low birth weight infants. *Nutrients*. 10:707. https://doi.org/10.3390/nu10060707

Mirpuri, J., M. Raetz, C.R. Sturge, C.L. Wilhelm, A. Benson, R.C. Savani, L.V. Hooper, and F. Yarovinsky. 2014. Proteobacteria-specific IgA regulates maturation of the intestinal microbiota. *Gut Microbes*. 5:28–39. https://doi.org/10.4161/gmic.26489

Moor, K., J. Fadlallah, A. Toska, D. Sterlin, M.L. Balmer, A.J. Macpherson, G. Gorochov, M. Larsen, and E. Slack. 2016. Analysis of bacterial-surface-specific antibodies in body fluids using bacterial flow cytometry. *Nat. Protoc.* 11:1531–1553. https://doi.org/10.1038/nprot.2016.091

Neu, J., and W.A. Walker. 2011. Necrotizing enterocolitis. *N. Engl. J. Med.* 364:255–264. https://doi.org/10.1056/NEJMra1005408

Niño, D.F., C.P. Sodhi, and D.J. Hackam. 2016. Necrotizing enterocolitis: New insights into pathogenesis and mechanisms. *Nat. Rev. Gastroenterol. Hepatol.* 13:590–600. https://doi.org/10.1038/nrgastro.2016.119

Oddy, W.H. 2017. Breastfeeding, childhood asthma, and allergic disease. *Ann. Nutr. Metab.* 70:26–36. https://doi.org/10.1159/000457920

Olm, M.R., N. Bhattacharya, A. Crits-Christoph, B.A. Firek, R. Baker, Y.S. Song, M.J. Morowitz, and J.F. Banfield. 2019. Necrotizing enterocolitis is preceded by increased gut bacterial replication, klebsiella, and fimbriae-encoding bacteria. *Sci. Adv.* 5:eaax5727. https://doi.org/10.1126/sciadv.aax5727

Pabst, O., and E. Slack. 2020. IgA and the intestinal microbiota: The importance of being specific. *Mucosal Immunol.* 13:12–21. https://doi.org/10.1038/s41385-019-0227-4

Pammi, M., J. Cope, P.I. Tarr, B.B. Warner, A.L. Morrow, V. Mai, K.E. Gregory, J.S. Kroll, V. McMurtry, M.J. Ferris, et al. 2017. Intestinal dysbiosis in preterm infants preceding necrotizing enterocolitis: A systematic review and meta-analysis. *Microbiome*. 5:31. https://doi.org/10.1186/s40168-017-0248-8

Pammi, M., and G. Suresh. 2017. Enteral lactoferrin supplementation for prevention of sepsis and necrotizing enterocolitis in preterm infants. *Cochrane Database Syst. Rev.* 6:CD007137. https://doi.org/10.1002/14651858.CD007137.pub5

Peila, C., G.E. Moro, E. Bertino, L. Cavallarin, M. Giribaldi, F. Giuliani, F. Cresi, and A. Coscia. 2016. The effect of holder pasteurization on nutrients and biologically-active components in donor human milk: A review. *Nutrients*. 8:477. https://doi.org/10.3390/nu8080477

Planer, J.D., Y. Peng, A.L. Kau, L.V. Blanton, I.M. Ndao, P.I. Tarr, B.B. Warner, and J.I. Gordon. 2016. Development of the gut microbiota and mucosal IgA responses in twins and gnotobiotic mice. *Nature*. 534:263–266. https://doi.org/10.1038/nature17940

Quigley, M., N.D. Embleton, and W. McGuire. 2018. Formula versus donor breast milk for feeding preterm or low birth weight infants. *Cochrane Database Syst. Rev.* 6:CD002971. https://doi.org/10.1002/14651858.CD002971.pub4

Ramanan, D., E. Sefik, S. Galván-Peña, M. Wu, L. Yang, Z. Yang, A. Kostic, T.V. Golovkina, D.L. Kasper, D. Mathis, and C. Benoist. 2020. An immunologic mode of multigenerational transmission governs a gut treg setpoint. *Cell*. 181:1276–1290.e13. https://doi.org/10.1016/j.cell.2020.04.030

Reyman, M., M.A. van Houten, D. van Baarle, A.A.T.M. Bosch, W.H. Man, M.L.J.N. Chu, K. Arp, R.L. Watson, E.A.M. Sanders, S. Fuentes, and D. Bogaert. 2019. Impact of delivery mode-associated gut microbiota dynamics on health in the first year of life. *Nat. Commun.* 10:4997. https://doi.org/10.1038/s41467-019-13014-7

Rogier, E.W., A.L. Frantz, M.E. Bruno, L. Wedlund, D.A. Cohen, A.J. Stromberg, and C.S. Kaetzel. 2014. Secretory antibodies in breast milk promote long-term intestinal homeostasis by regulating the gut microbiota and host gene expression. *Proc. Natl. Acad. Sci. USA*. 111:3074–3079. https://doi.org/10.1073/pnas.1315792111

Rognum, T.O., S. Thrane, L. Stoltenberg, A. Vege, and P. Brandtzaeg. 1992. Development of intestinal mucosal immunity in fetal life and the first postnatal months. *Pediatr. Res.* 32:145–149. https://doi.org/10.1203/00006450-199208000-00003

Rollenske, T., V. Szijarto, J. Lukasiewicz, L.M. Guachalla, K. Stojkovic, K. Hartl, L. Stulik, S. Kocher, F. Lasitschka, M. Al-Saeedi, et al. 2018. Cross-specificity of protective human antibodies against Klebsiella pneumoniae LPS O-antigen. *Nat. Immunol.* 19:617–624. https://doi.org/10.1038/s41590-018-0106-2

Roux, M.E., M. McWilliams, J.M. Phillips-Quagliata, P. Weisz-Carrington, and M.E. Lamm. 1977. Origin of IgA-secreting plasma cells in the mammary gland. *J. Exp. Med.* 146:1311–1322. https://doi.org/10.1084/jem.146.5.1311

Sandin, C., S. Linse, T. Areschoug, J.M. Woof, J. Reinholdt, and G. Lindahl. 2002. Isolation and detection of human IgA using a streptococcal IgA-binding peptide. *J. Immunol.* 169:1357–1364. https://doi.org/10.4049/jimmunol.169.3.1357

Slack, E., S. Hapfelmeier, B. Stecher, Y. Velykoredko, M. Stoel, M.A. Lawson, M.B. Geuking, B. Beutler, T.F. Tedder, W.D. Hardt, et al. 2009. Innate and adaptive immunity cooperate flexibly to maintain host-microbiota mutualism. *Science*. 325:617–620. https://doi.org/10.1126/science.1172747

Sobti, J., G.P. Mathur, A. Gupta, and WHO. 2002. WHO's proposed global strategy for infant and young child feeding: A viewpoint. *J. Indian Med. Assoc.* 100:502–504: 506.

Suscovich, T.J., J.K. Fallon, J. Das, A.R. Demas, J. Crain, C.H. Linde, A. Michell, H. Natarajan, C. Arevalo, T. Broge, et al. 2020. Mapping functional humoral correlates of protection against malaria challenge following RTS,S/AS01 vaccination. *Sci. Transl. Med.* 12:eabb4757. https://doi.org/10.1126/scitranslmed.abb4757

Walker, W.A., and R.S. Iyengar. 2015. Breast milk, microbiota, and intestinal immune homeostasis. *Pediatr. Res.* 77:220–228. https://doi.org/10.1038/pr.2014.160

Warner, B.B., and P.I. Tarr. 2016. Necrotizing enterocolitis and preterm infant gut bacteria. *Semin. Fetal Neonatal. Med.* 21:394–399. https://doi.org/10.1016/j.siny.2016.06.001

Wilson, E., and E.C. Butcher. 2004. CCL28 controls immunoglobulin (Ig)A plasma cell accumulation in the lactating mammary gland and IgA antibody transfer to the neonate. *J. Exp. Med.* 200:805–809. https://doi.org/10.1084/jem.20041069

Yang, Y., and N.W. Palm. 2020. Immunoglobulin A and the microbiome. *Curr. Opin. Microbiol.* 56:89–96. https://doi.org/10.1016/j.mib.2020.08.003

Yu, X., M. Duval, C. Lewis, M.A. Gawron, R. Wang, M.R. Posner, and L.A. Cavacini. 2013. Impact of IgA constant domain on HIV-1 neutralizing function of monoclonal antibody F425A1g8. *J. Immunol.* 190:205–210. https://doi.org/10.4049/jimmunol.1201469

Zhang, W., Q. Feng, C. Wang, X. Zeng, Y. Du, L. Lin, J. Wu, L. Fu, K. Yang, X. Xu, et al. 2017. Characterization of the B cell receptor repertoire in the intestinal mucosa and of tumor-infiltrating lymphocytes in colorectal adenoma and carcinoma. *J. Immunol.* 198:3719–3728. https://doi.org/10.4049/jimmunol.1602039

Zikan, J., J. Novotny, T.L. Trapane, M.E. Koshland, D.W. Urry, J.C. Bennett, and J. Mestecky. 1985. Secondary structure of the immunoglobulin J chain. *Proc. Natl. Acad. Sci. USA*. 82:5905–5909. https://doi.org/10.1073/pnas.82.17.5905

Supplemental material

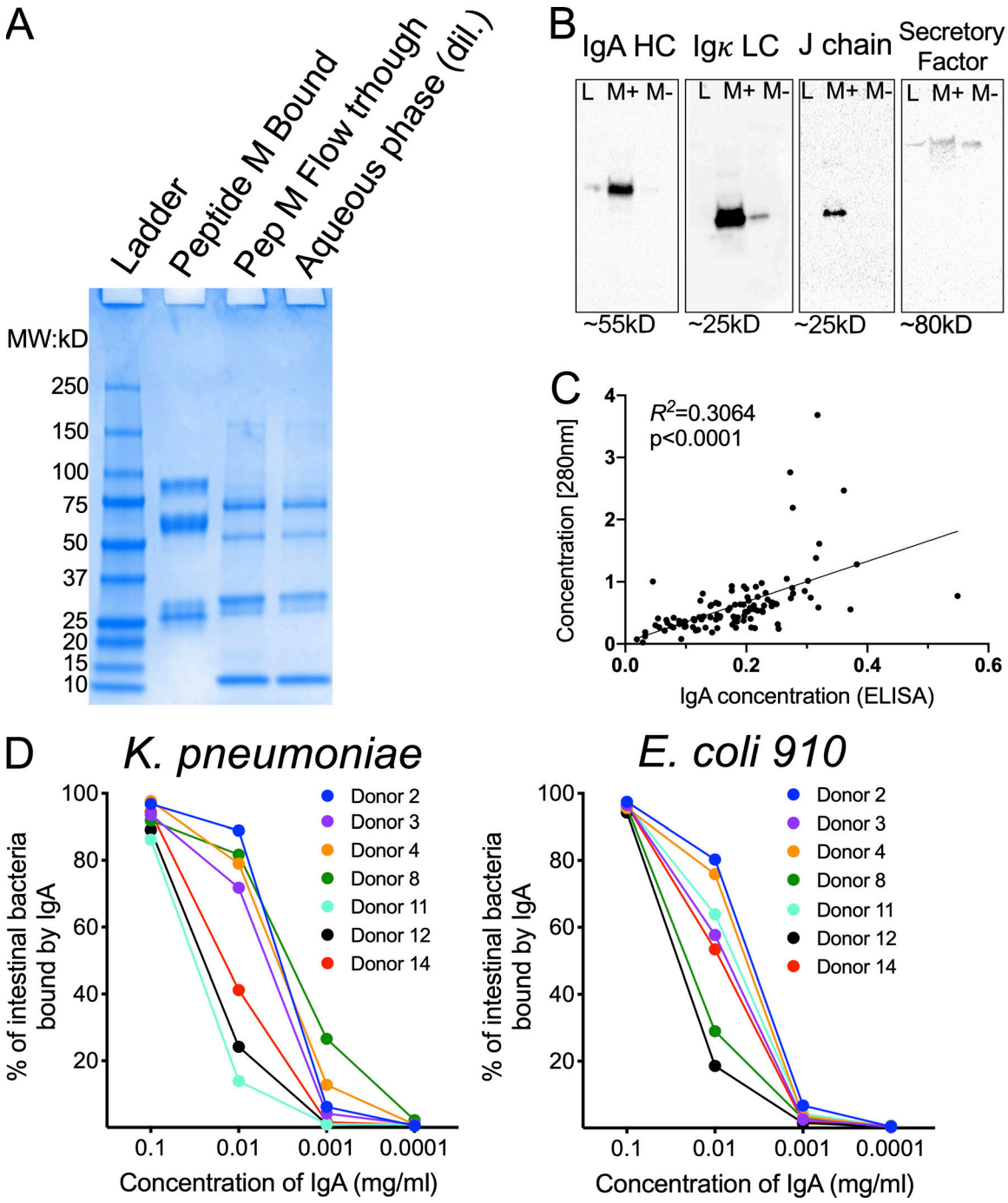

Figure S1. **Isolation of IgA from breast milk by Peptide M columns substantially enriches for secretory IgA. (A)** The soluble fraction of a breast milk sample was run over a Peptide M column and analyzed on an LDS-PAGE gel. Shown are the Peptide M bound fraction, the flow through, and the aqueous phase prior to separation. MW, molecular weight. **(B)** LDS-PAGE gels were prepared as in A, transferred to nitrocellulose, and blotted with antibodies to different proteins as described above the blot. L = ladder; M+ = Peptide M bound fraction and M− = flow through of Peptide M column. **(C)** Concordance of IgA estimations made my 280 nm light absorbance and IgA ELISA. **(D)** 10-fold dilutions of Peptide M purified IgA fractions run over the flow cytometric array as described in Fig. 1 A. Shown are two example bacteria. A and B are one example of two separate experiments. C is the aggregate of all of the donor samples used in the manuscript. D was performed once. Source data are available for this figure: SourceData FS1.

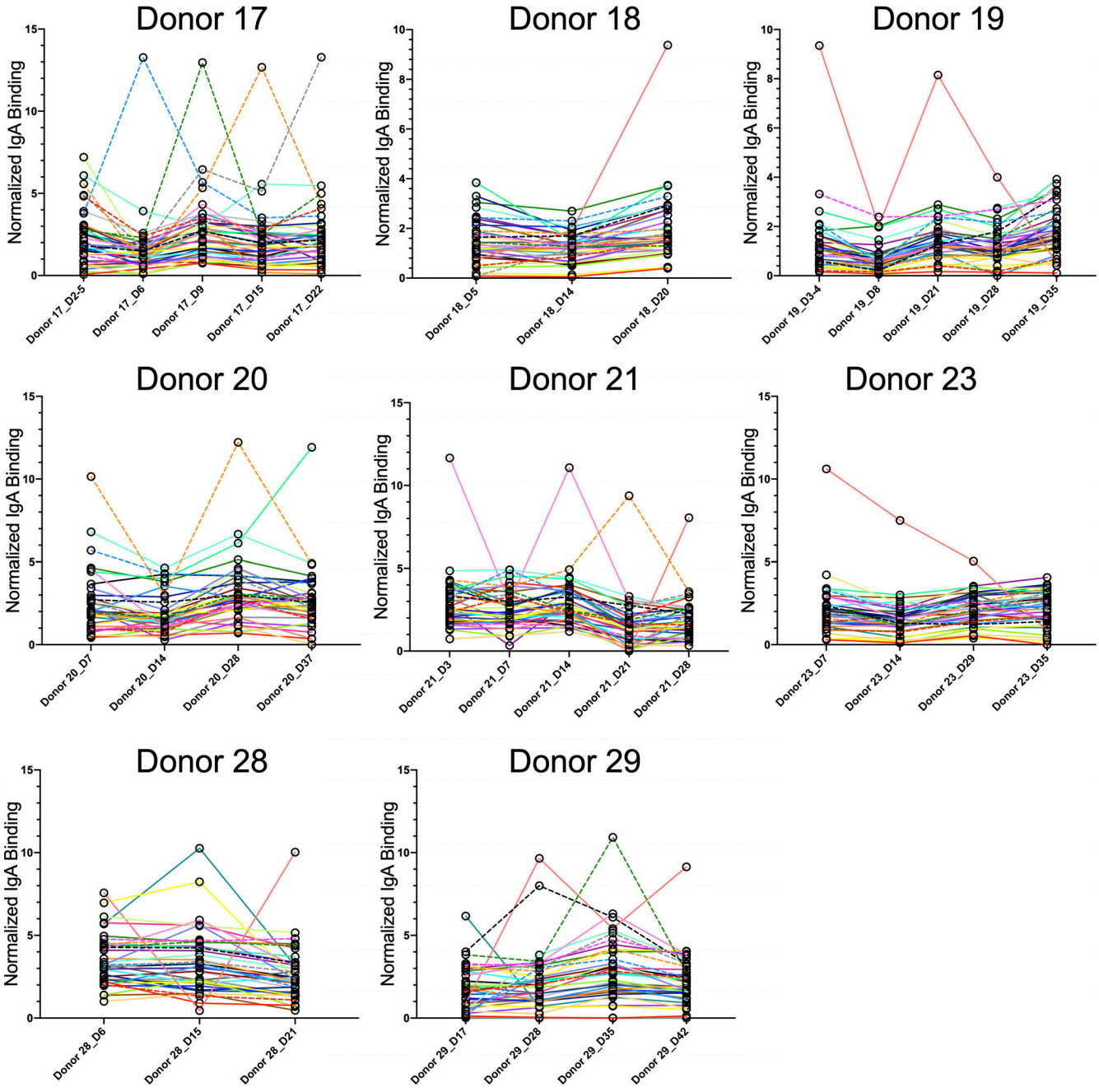

Figure S2. **Longitudinal analysis of the antibaterial IgA response from sequentially collected breast milk samples.** Graph of normalized IgA binding to all bacterial types from longitudinal milk samples. Samples from each donor are in order left to right. Each donor is represented by an individual graph and each bacteria by a different colored line. This experiment was performed once.

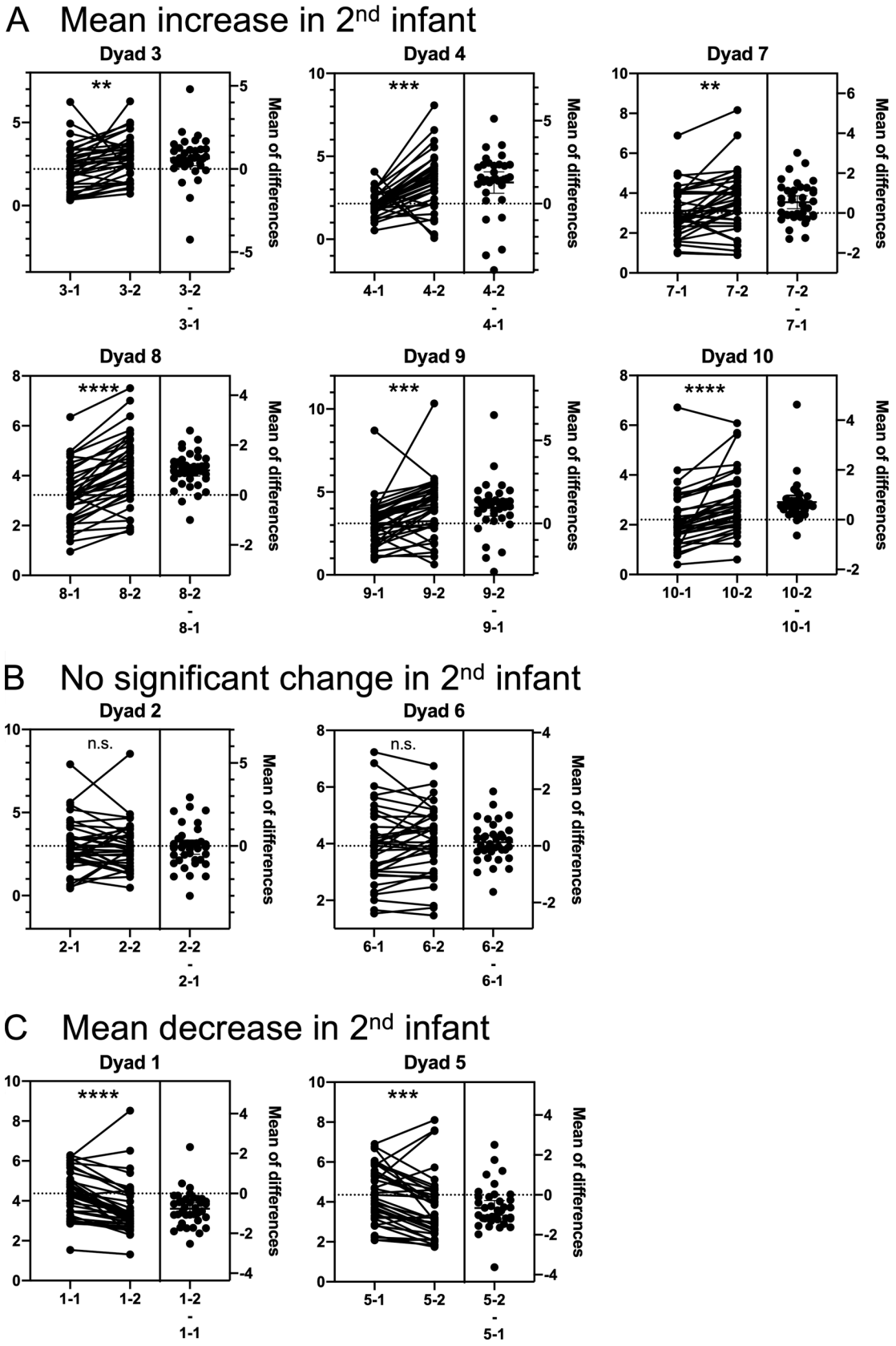

Figure S3. **Detailed comparisons of the antibacterial IgA reactivity from donors collected over two separate infants.** Paired Student's *t* tests comparing the antibacterial IgA binding between breast milk collected from the first and second infant. Each dot represents a different bacterial taxon and each graph is a different donor dyad (as indicated). The right-hand graph is the difference (norm. IgA binding infant 2 – norm. IgA binding infant 1) for each taxon. This experiment was performed once.

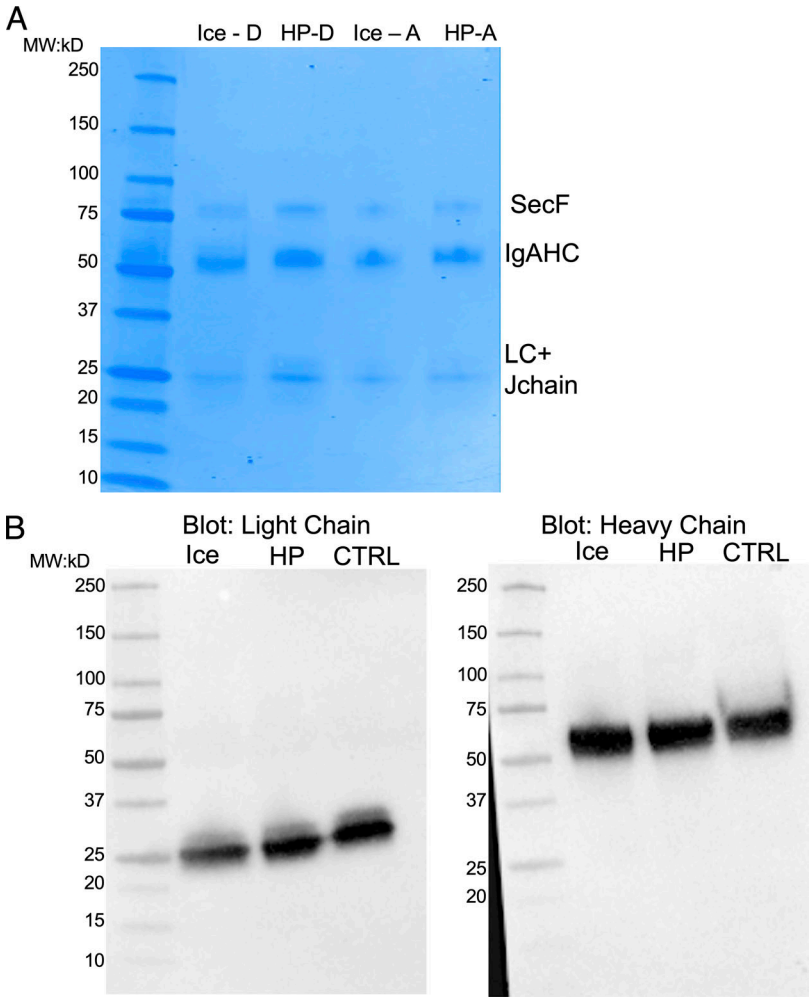

Figure S4. **Effect of pasteurization on different antibody components.** Two breast milk samples (A and D) were thawed and IgA isolated by passage over a Peptide M column. Each sample was split in two then treated by Holder pasteurization (62.5°C for 30 min) or left on ice for 30 min. Control samples were used just after Peptide M isolation. **(A)** Samples were boiled in Laemmli buffer and run on an LDS-PAGE gel (4–15% Gradient Acrylamide gel). Samples were normalized to protein content after pasteurization. **(B)** "D" samples were transferred onto nitrocellulose and blotted for heavy chain (right) or light chain (kappa; left). Samples were normalized to protein content after pasteurization. HP, Holder pasteurization; Ctrl, no treatment; SecF, SeF; IgAHC, IgA heavy chain; LC, light chain; MW, molecular weight. Source data are available for this figure: SourceData FS4